Behaviour of cellular structures with fluid fillers under impact loading

Matej Vesenjak[1], Andreas Öchsner[2], Matjaz Hribersek[3], Zoran Ren[4]

[1] University of Maribor, Faculty of Mechanical Engineering, Smetanova 17, 2000 Maribor, Slovenia, e-mail: m.vesenjak@uni-mb.si

[2] University of Aveiro, Department of Mechanical Engineering, 3810-193 Aveiro, Portugal, e-mail: aoechsner@mec.ua.pt

[3] University of Maribor, Faculty of Mechanical Engineering, Smetanova 17, 2000 Maribor, Slovenia, e-mail: matjaz.hribersek@guest.arnes.si

[4] University of Maribor, Faculty of Mechanical Engineering, Smetanova 17, 2000 Maribor, Slovenia, e-mail: ren@uni-mb.si

ABSTRACT:

The paper investigates the behaviour of closed- and open-cell cellular structures under uniaxial impact loading by means of computational simulations using the explicit nonlinear finite element code LS-DYNA. Simulations also consider the influence of pore fillers and the base material strain rate sensitivity. The behaviour of closed-cell cellular structure has been evaluated with use of the representative volume element, where the influence of residual gas inside the closed pores has been studied. Open-cell cellular structure was modelled as a whole to properly account for considered fluid flow through the cells, which significantly influences macroscopic behaviour of the cellular structure. The fluid has been modelled by applying a meshless Smoothed Particle Hydrodynamics (SPH) method. Parametric computational simulations provide grounds for optimization of cellular structures to satisfy different requirements, which makes them very attractive for use in general engineering applications.

Keywords: Cellular structure, Open cells, Closed cells, Pore filler, Computational simulations, Fully coupled fluid-structure interaction, FEM, SPH.

1 INTRODUCTION

Materials with cellular structures are arousing great interest in modern engineering industry due to their favourable mechanical and thermal properties. To employ the advantages of these structures for general engineering applications their development was enforced worldwide in the past couple of years (Figure 1). The fundamental properties of the metallic foams and metallic hollow sphere structures are low density accompanied with high strength and stiffness, good damping and energy absorbing capabilities, non flammability and a possibility of cellular structure optimization to meet certain application demands. However, for successful use of this new class of materials a detailed knowledge of their mechanical properties is required [1].

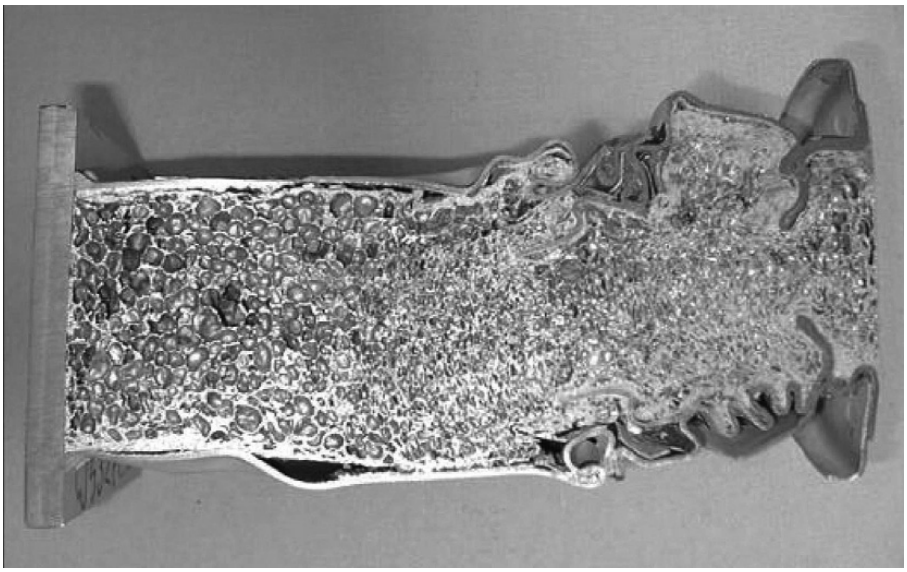

Figure 1 Longitudinal crash absorber with cellular internal structure [2]

The purpose of the presented research study is characterisation of new advanced cellular materials with pore fillers under impact loading conditions considering high strain rates and large deformations. The computational models of regular closed- and open-cell cellular structures have been evaluated and validated. The base material properties have been determined with experimental measurements of specimens under quasi-static and dynamic uniaxial loading conditions. The computational models account for the fully coupled interaction between the base material and the pore filler. In this study cellular structures with various base materials and relative densities are studied, whereas fillers with different viscosities are also considered. The influence of gas trapped inside the closed-cell cellular structure has been analysed with the representative volume element. The analysis of the viscous filler inside the pores of the open-cell cellular structures has been performed with the combination of the finite element method and the meshless method Smoothed particle hydrodynamics. The LS-DYNA code has been used to perform dynamic computational simulations.

2 CELLULAR MATERIALS

Cellular structures have an attractive combination of physical and mechanical properties and are being increasingly used in modern engineering applications. Research of their behaviour under quasi-static and high strain rates is valuable for engineering applications such as those related to impact and energy absorption. Usually cellular material is divided in two groups regarding the cell morphology: (i) open-cell and (ii) closed-cell (Figure 2). In the open-cell cellular structures beams form the cell struts and in closed-cell cellular structure the closed cells are distributed in the base materials enclosed by cell surfaces [3].

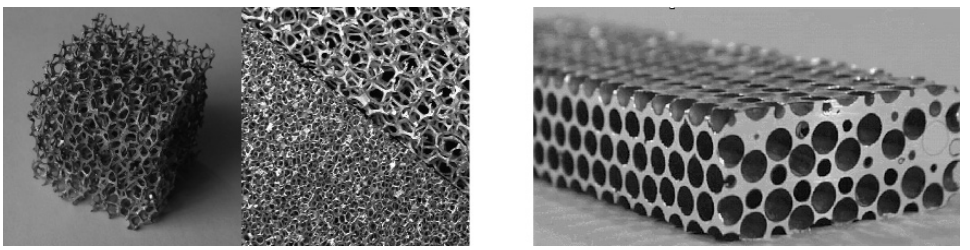

Figure 2 Open-cell (foam, DUOCEL® - left) and closed-cell cellular metals (right, [4])

Their mechanical behaviour mainly depends on the relative density (the density of the cellular structure, divided by the base material density) and the base material which can vary between metals, plastics, glass and ceramics [3]. The other important parameters of the cellular structures are geometry and topology (regular or irregular structure) and possible filler type. To achieve adequate properties of the cellular material, the base material has to be carefully chosen in regard to its mechanical (strength, stiffness) and thermal properties (thermal conductivity). The advantages of cellular materials in general are low density (light-weight structures), high acoustic isolation and damping, hydrophobic (low water absorption), relatively high grade of deformation, relatively high energy absorption, durability at dynamic loadings and fatigue, recyclability [5].

However, there are technological problems related to the control of the material structure, since the majority of existing technologies do not allow for precise control of the shape, size and distribution of the cellular pores [4, 6]. This results in wide scatter of physical and other characteristics of these materials and components. Therefore additional research is being conducted to better understand the stabilizing mechanisms effective during foaming in a molten state. The purpose is to establish the basis for the production of foams with smaller and more homogenous cell sizes. A number of alternative production processes based on the use of templates have also been developed in recent years.

With regard to material characteristics, particular emphasis is being placed on elucidating the correlation between strength and cell structure. The goal is to develop numerical and analytical simulation processes which make material behaviour predictable [1]. Recently developed fabrication methods for hollow sphere structures or lotus-type porous metals result in more homogeneous pore structures [4, 6, 7, 8]. First experimental investigations preformed by Anderson et al. [9] show that the mechanical material properties of comparable samples seem to be entirely reproducible. However, behaviour of cellular materials in different applications, when subjected to an inhomogeneous loading field, is not well understood yet [10]. Such inhomogeneous loading usually occurs at notches and holes. Nevertheless, the micro- and macroscopic properties of cellular materials make them very attractive for use in automotive, rail, naval and aerospace industry as heat exchangers, filters, bearings, acoustic dampers, core material in sandwich structures, bio-medical implants and elements for energy absorption [5, 11, 12]. One of the most important areas for the future application of cellular materials is in the automotive industry, where their high impact energy absorption through deformation is of crucial importance for increasing passive safety of vehicles [5, 11].

The basic mechanical and thermal properties of cellular materials have been closely examined by Gibson and Ashby [11] and their behaviour under high strain rates was examined e.g. by Deshpande and Fleck [13]. The state-of-the-art review of development,

manufacturing, characterisation and application of metal foams has been given by Banhart [5]. The general mechanical properties of cellular materials are analysed in detail by Sieradzki et al. [14] and Papadopoulos et al. [15], their composition and application in [16, 17, 18, 19] and the manufacturing by Gibson et al. [11] and in [20]. Several design guidelines are presented by Ashby et al. [21]. The internet site Metal foam info mediates up-to-date information about cellular structures in general, but is focused mostly on metallic foams [22].

Cellular materials have a characteristic stress-strain relationship in compression, which can be divided into four main areas:

a) quasi-static linear response,
b) transition zone,
c) stress plateau and
d) densification.

After initial quasi-linear elastic response, where the elastic deformation of the cell walls occurs, the cellular materials first experience buckling, plastic deformation and collapse of intercellular walls in the transition zone. Under further loading the mechanism of buckling and collapse becomes even more pronounced, which is manifested in large strains at almost constant stress (stress plateau) until the cells completely collapse (densification). At this point the cellular material stiffness increases and consequently converges towards the stiffness of the base material. During tensile loading the linear elastic response remains the same as at compressive loading, according to Gibson [23]. Additionally, with the strain increase, the cells become more orientated with the loading direction, increasing the stiffness of the cellular material until the tensile failure. The mechanism of cell deformation and collapse also depends on the cellular structure relative density. While the cell walls are subjected to buckling and bending at low relative densities, they shear at higher relative densities since the cell walls are too short and/or too thick to bend [3].

The cellular material is able to absorb significant amount of energy through its deformation during the loading process. The absorbed energy is a sum of energy accumulated during elastic deformation and energy absorbed by the plastic deformation. The latter is very important for crash energy absorption and is more pronounced for metal foams than for polymers. It is worth noting that the energy absorption is also strain-rate dependent. The higher the strain-rate, the higher is the capability of energy absorption through deformation.

3 PORE FILLERS

During the manufacturing procedure of closed-cell cellular metals with gas injection (air, CO_2, O_2, Ar) the gas in pores can reach up to 1200 K and 100 MPa according to Elzey et al. [24] and Öchsner et al. [25]. After solidification and cooling down it can be assumed that the gas is trapped in the base material for a certain time. During impact loading of such materials the gas inside the pores might significantly influence the macroscopic cellular material behaviour. High gas compression under impact loading causes significant gas temperature increase, which influences the overall response of the cellular material that might result in inadvertent collapse of intercellular walls and increase of the material structure porosity [26, 27]. Even for open-cell honeycomb structures it was reported by Shkolnikov that the gas inside the pores contributed to 10 % higher stiffness of the honeycomb, although this effect was observed only for larger specimens [28].

Investigations to incorporate the gas influence on macroscopic mechanical behaviour were done by Kitazono et al. [29], where the authors have in their analytical approach assumed a constant gas pressure in closed pore structure. However, this approach did not

consider the change of the gas pressure during the deformation and the concept of large plastic deformation. Therefore, the application of their model is limited to time-independent, small deformations problems. Under compressive loading the pore gas pressure increases due to cell deformation, thus contributing to structure stiffness increase up to the point of base material yielding. This results in the collapse of intercellular walls and increase of the material structure porosity [24]. Öchsner et al. have shown a strong effect on the yield stress due to varying pore gas pressure under quasi-static loading and isothermal conditions. More pronounced influence can be therefore expected for the case of impact loading [25].

Cellular materials are commonly used in shock absorption applications. Their structure enables to minimize the collision damage by impact energy dissipation during the deformation and reducing transmitted forces to higher safety levels [30]. Fluid (usually a gas) in these empty pores is compressed and flows through the cells during the loading process. Shim and Yap [31] state that this effect might be neglected in cellular materials with low relative density and slow deformation (low strain rates). Consequently, it might be neglected at quasi-static mechanical testing of cellular materials to determine their mechanical properties. However, the effect of gaseous or even liquid fillers increases with higher strain rates. This results in change of yielding and hardening under dynamic loading conditions and results in a necessity to consider the strain-rate sensitivity for cellular materials. The effect of strong strain-rate dependence was already observed by Ohrndorf et al. [26], by studying mechanical properties of closed-cell structures at translational strain rates up to 2 s^{-1}. It was concluded that the cellular materials have significantly different stress-strain relationship at higher strain-rates without the characteristic plateau stress. Generally, the capability of impact energy absorption increases with increasing strain-rate sensitivity. It should be noted that the strain-rate sensitivity is also temperature dependent [32].

Very fast deformation at high strain rates results in temperature change of the base material, which affects its mechanical properties. However, for impact loading the loading time might be short enough to justify neglecting the temperature effects by heat conduction in the base material. The subsequent temperature increase after the impact is in this case not important. Preliminary simulations based on transient heat transfer simulations in two-dimensional computational model of closed-cell cellular structures, accounting for different relative densities and pore fillers, seem to justify this assumption [33].

In open-cell cellular materials the gas can not be trapped in the cellular structure without sealing of the material boundary. A logical solution to increase the energy absorption in open-cell cellular materials is by filling the cellular structure with viscous fluid. Such fluid offers certain level of flow resistance during collapse of cellular structure due to its viscosity, which in turn increases the structure stiffness during the deformation process. Preliminary investigations have shown that in combination with high strain-rate loading this result in substantial increase of energy absorption [27, 34]. Experimental testing and computational simulations carried out have already shown that the filler significantly influences the macroscopic behaviour of materials with open-cell cellular structure [34]. Therefore it is reasonable to investigate and examine further the filler influence with additional experimental testing and computational simulations in order to determine advanced numerical models that will assure a fast, accurate and reliable method for use in general engineering.

However, a successful computational simulation of the cellular material behaviour under influence of external loading necessitates use of suitable numerical and constitutive models. Some of these models have been developed in the past, but they are limited regarding the

loading velocity and do not account for possible cell filler influence on the macroscopic properties of the cellular material [13, 35, 36, 37, 38].

Therefore, it is reasonable to investigate the combination of cellular structures with filler by determining its influence on the macroscopic behaviour of cellular metals by means of computational simulations. Parametric computational simulations of the closed- and open-cell cellular structure under impact conditions with gaseous and liquid fillers were performed in this respect.

4 CLOSED-CELL CELLULAR STRUCTURES

Mechanical characterisation of closed-cell cellular structures with experimental testing is usually limited to macroscopic cellular material behaviour, since it is not possible to measure the change of the internal pore gas pressure and its influence. Therefore dynamic computational simulations of closed-cell cellular structure have been used in order to evaluate the influence of the gaseous pore filler at different relative densities.

4.1 COMPUTATIONAL MODEL

Complete detailed modelling of cellular materials is usually not possible due to insufficient computer capabilities. For this reason the cellular materials are often modelled by considering a "representative volume element", which serves for detailed studies of mechanical behaviour of a minimum number of unit cells and its mathematical characterization, which is then used as a cellular material constitutive model in consequent computational analyses of complete cellular structure. The minimum number of unit cells must be sufficient to correctly represent macroscopic parameters of the cellular material [34, 39]. In this a regular cellular structure has been considered to achieve reasonable computational times (Figure 3).

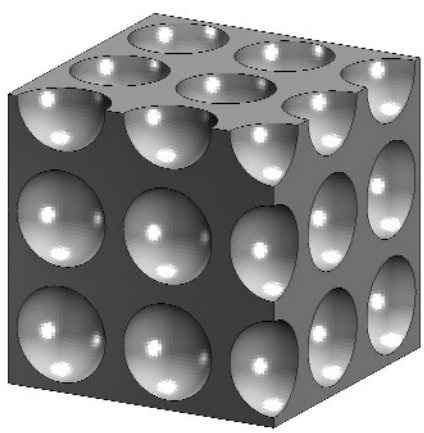

Figure 3 Regular cellular structure

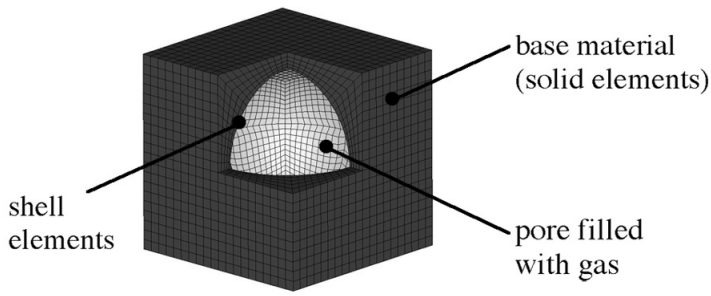

Figure 4 Representative volume element

The representative volume element was cube-shaped with the edges varying from 1.523 to 2.605 mm in length and a spherical pore with a radius of 0.75 mm which corresponded to relative densities varying from 0.5 to 0.9 (Figure 4). The lowest possible relative density of the considered cell geometry and topology is 0.48.

Aluminium alloy AlCuMg1 has been used as the base material of closed-cell cellular structure [39]. The strain rate sensitivity was considered by implementing the Cowper-Symonds' constitutive relation

$$\frac{\sigma'}{\sigma} = 1 + \left(\frac{\dot{\varepsilon}}{C}\right)^{1/p}, \tag{1}$$

where σ' is the stress at the strain rate $\dot{\varepsilon}$ and σ is the stress at quasi-static conditions. C and p are material parameters which characterize the material strain rate sensitivity [40, 41, 42]. The mechanical properties of the base material are listed in Table 1.

Table 1. Mechanical properties of the aluminium alloy AlCuMg1

Density	**Young's modulus**	**Poisson ratio**	**Yield stress**	**Cowper-Symonds' parameters**	
ρ_0	E	υ	Re	C	p
[kg/m^3]	[GPa]	[-]	[MPa]	[s^{-1}]	[-]
2,700	72.0	0.3	301	6,500	4

The base material was meshed with fully integrated 8-node brick elements. With additional parametrical simulations a proper mesh density and time step were evaluated to achieve precise results and reasonable computational times.

Two gases (Air and CO_2) have been considered in the computational models, with their properties listed in Table 2.

Table 2. Gas properties

Gas	Density	Spec. heat coeff. at const. volume	Spec. heat coeff. at const. pressure	Initial temperature	Initial pressure
	ρ	c_v	c_p	T_0	p_0
	[kg/m^3]	[J/kg K]	[J/kg K]	[K]	[MPa]
Air	1.189	717	1,005	293	0.1
CO_2	1.977	631	820	293	0.1

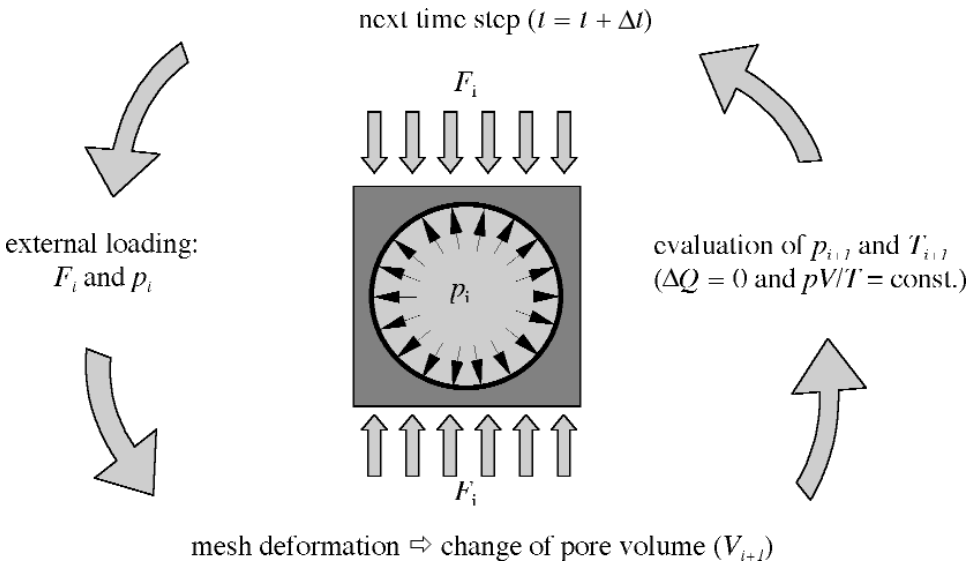

Figure 5 Interaction between the base material and the pore gas

A fully coupled fluid-structure interaction between the base material and the pore filler (gas), accounting for actual base material deformation and change of gas pressure, temperature and its volume has been considered. A special formulation (airbag definition) in the LS-DYNA code was used to consider the gas influence inside the pore and to compute its pressure, volume and temperature change [40, 44]. It was presumed that the gas has ideal properties (pV/T = const.). With additional simulations it was proven that it is very important to consider the change of temperature (not only pV = const.) which contributes to the pore gas pressure build-up. The surface of the pore was meshed with shell elements of negligible stiffness (ρ = 1,000 kg/m^3, E = 1,000 MPa, ν = 0.3 and the thickness of shell elements was 0.1 mm) to properly define the used airbag model. The nodes of the shell elements were coincident with the inner surface nodes of the base material. The deformation of the structure

(change of the pore volume) thus resulted in change of gas temperature and pressure acting on the structure, which is schematically presented in Figure 5.

Four different initial pore gas pressures of 0.5, 5, 50 and 100 MPa were used to study its influence on the macroscopic behaviour of the cellular material.

The impact load was displacement controlled and applied to the upper surface of the cell with prescribed strain rate of 100 s^{-1}. Two load cases were considered: (i) compressive and (ii) tensile loading. The lower surface was fixed in the vertical direction. Special periodic boundary conditions were prescribed on side surfaces, where all nodes on a surface have the same displacement in the normal direction to the surface [39]. Those boundary conditions have been also confirmed with parametrical simulations [34, 43].

The pore surface elements were defined as one contact group to account for possible self-contact at very large deformations.

The analysis time interval was set to 10 ms, with results output required every 0.001 ms. In the first millisecond the cellular structure was pre-stressed with gas pressure build-up to prescribed level. After that initialization time the structure was exposed to mechanical impact loading.

The average size of the elements is 0.05 mm and the whole model consists of 12,000 brick elements and 2,400 shell elements, together contributing to 85,200 degrees of freedom. The time step for explicit transient dynamic analysis was automatically set to 0.1 ms with regard to the lowest resonant frequency of the structure. The analyses were run on a PC-cluster of 8 units with Intel Pentium IV 3200 MHz processors and 1 GB RAM each and a single run lasted for approximately 170 minutes.

4.2 RESULTS

Due to the initial pore gas pressure (0.5, 5, 50 and 100 MPa) the base material is pre-stressed to a certain level before the mechanical loading starts (Table 3).

Table 3. Initial stress in the base material due to initial pore gas pressure

Initial gas pressure	MPa	0.5	5	50	100
Max $\sigma_{\text{von Mises}}$	MPa	1.4	14	155	230

The stress in the base material also depends on the relative density and increases with decreasing the relative density.

Figures 6 and 7 illustrate the difference between cell deformations at lower and higher initial pore gas pressure. As expected, the pore compresses more in the case of lower initial pore gas pressure than in the case of higher pore gas pressure. High pore gas pressure also results in higher base material deformation.

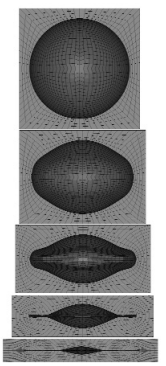

Figure 6 Cell deformation under compressive loading pore gas pressure of 0.5 MPa

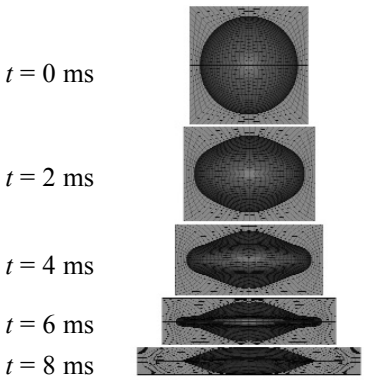

Figure 7 Cell deformation under compressive loading with with initial initial pore gas pressure of 100 MPa

Figure 8 illustrates the simulated behaviour of the closed-cell cellular structure under compressive and tensile impact loading with different initial pore gas pressures at a strain rate of 100 s^{-1}. Under compressive loading the pore volume decreases and consequently the internal pore gas pressure increases, see Figure 9. This mechanism leads to increase of the macroscopic yield stress (e.g. increase of 10.6 % for considered example, Figure 9), since the gas pressure inside the pore acts in the opposite direction than the external loading. With higher pore gas pressure the cellular structure exhibits higher stress levels during the plastic deformation and thus absorbs more impact energy. Furthermore, higher pore gas pressure contributes to delayed and slower densification of the cellular structure, which occurs at a higher strain. During tensile loading the higher pore gas pressure lowers the macroscopic yield stress (e.g. decrease of 18.7 % for considered example, Figure 10). With higher pore gas pressure the cellular structure exhibits lower stress levels during the plastic deformation and thus absorbs less impact energy, Figure 10.

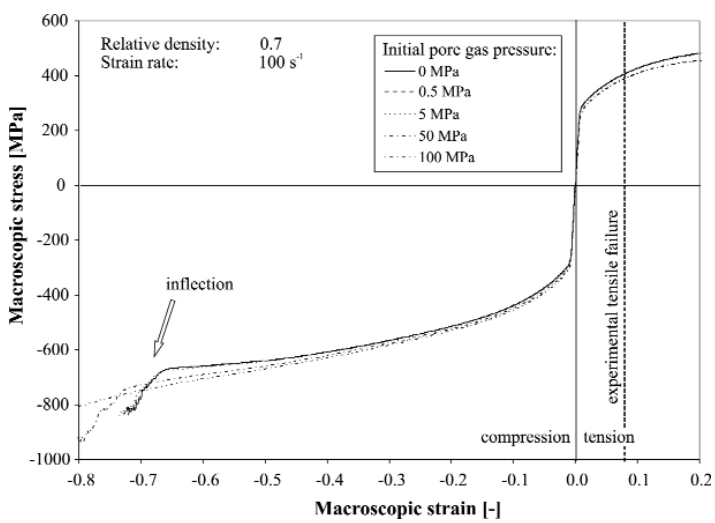

Figure 8 Influence of the gaseous filler

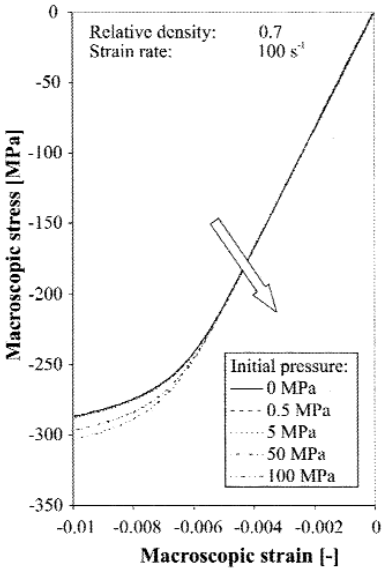

Figure 9: Compressive loading

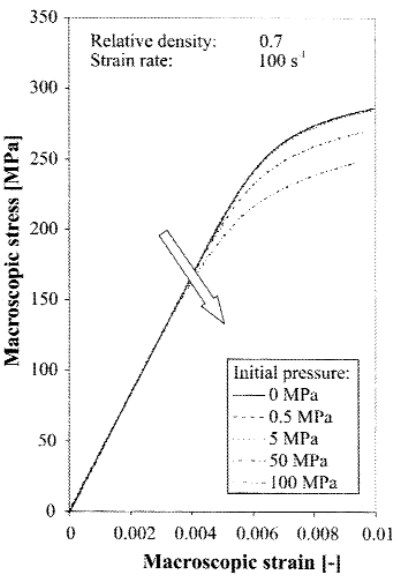

Figure 10: Tensile loading

Figure 9 Compressive loading Figure 10 Tensile loading

The relative gas pressure change in regard to the initial pore gas pressure for the relative density 0.7 is shown in Figure 11. It is evident that the gas pressure change is higher in case of a lower initial pressure. The diagram also confirms that the gas pressure rises up to a certain limit value that depends on the mechanical properties of the base material [34].

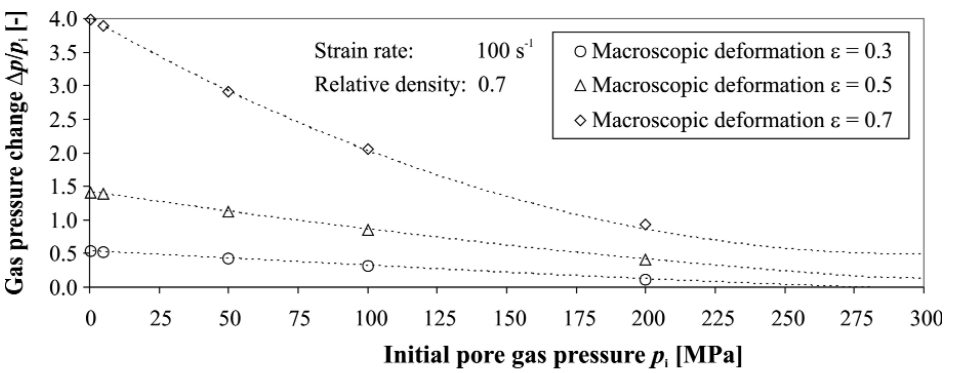

Figure 11 Relative gas pressure change regarding the initial pore gas pressure

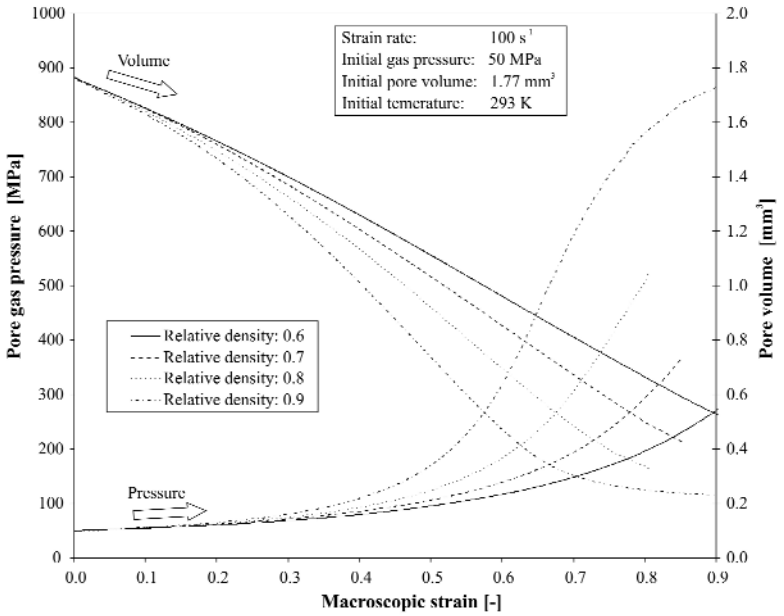

Figure 12 Change of pore volume and gas pressure at compressive loading for different relative densities

The change of gas pressure and pore volume at compressive loading for different relative densities is presented in Figure 12. The pore volume of the cellular structure with higher relative density is reduced more than in cellular structures with lower relative density, which is attributed to higher base material resistance. The pore gas pressures are therefore higher in cellular structures with higher relative density. A similar effect can be found when comparing base materials with different stiffness.

The macroscopic behaviour of cellular structure accounting for pore filler with different relative densities is shown in Figure 13. The influence of initial pore gas pressure is more pronounced in the cellular structure with relative density 0.6. From computed results it can be concluded that the pore gas pressure has higher influence on cellular structures with lower relative density.

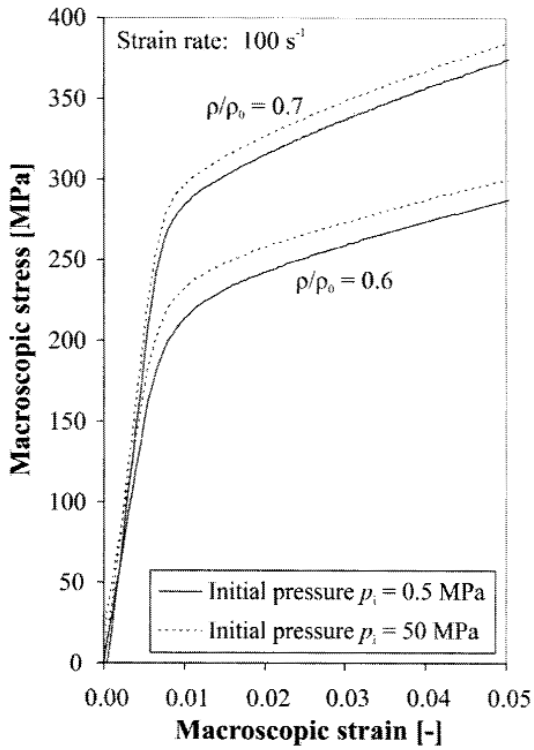

Figure 13 Influence of the pore gas at different relative densities

The influence of initial pore gas pressure at different strain rates for the closed-cell cellular structure with the relative density 0.7 is shown in Figure 14. Higher gas pressure increase at higher strain rates is evident, which can be attributed to higher base material strain rate sensitivity. However, the influence of different initial pore gas pressures on the global cellular structure behaviour is negligible at considered strain rates.

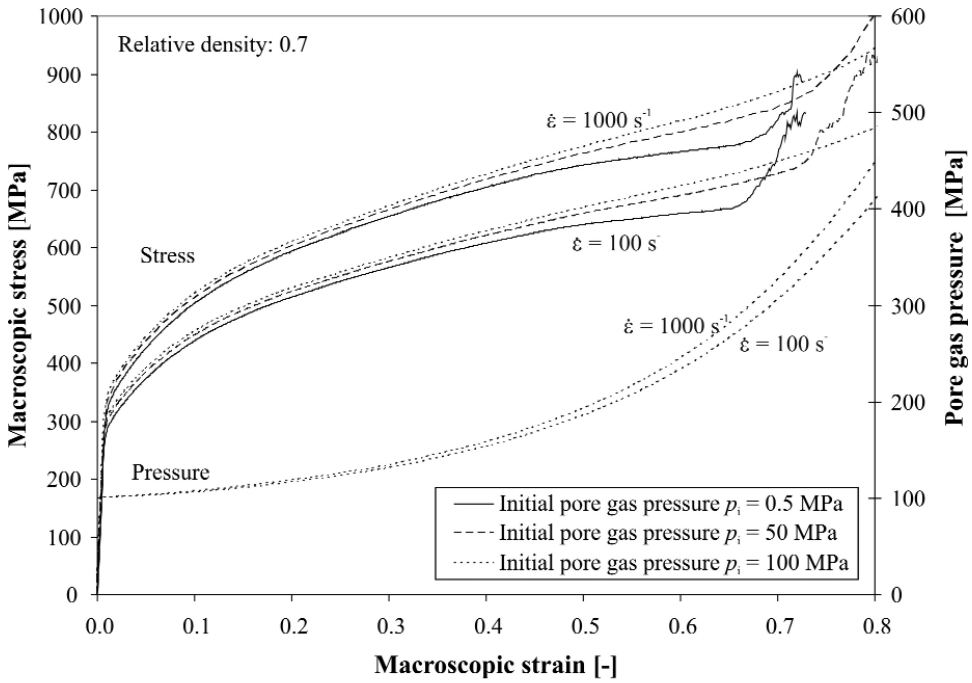

Figure 14 Influence of pore gas and strain rate

With additional computational simulations it was observed that the influence of filler gas type (air, CO_2) is negligible. However, at very low relative densities the type of the filler gas might have more pronounced effect on the global cellular structure response.

5 OPEN-CELL CELLULAR STRUCTURES

Initial experimental testing of regular open-cell cellular structures made of aluminium alloy showed a very brittle and unpredictable deformation [34]. Therefore viscous pore fillers have been introduced to improve the behaviour during the plastic deformation and increase the capability of deformational energy absorption. Computational simulations were carried out to investigate the influence and flow of the viscous pore filler more precisely.

5.1 COMPUTATIONAL MODEL OF THE STRUCTURE

The behaviour of open-cell cellular structures accounting for viscous fluid pore filler was studied for the case of regular and periodic pore geometry (Figure 15). In comparison with closed-cell cellular structure, the representative volume element approach could not be applied here since the filler flow through the cell could not be correctly described and simulated. The open-cell cellular structures with relative densities ρ/ρ_0 = 0.37; 0.27 and 0.16 which corresponds to the basic geometry dimensions of d = 3 mm and a = 4.5, 4.0 and 3.5 mm was considered in this computational study.

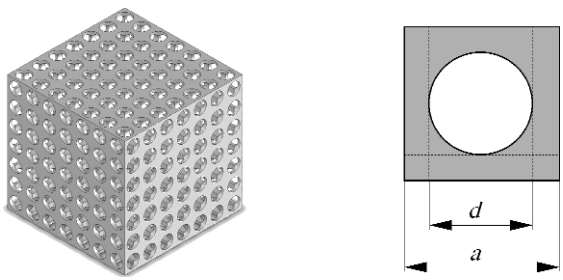

Figure 15 Geometry of the open-cell cellular structure

The polymer FullCure with different mechanical properties for the tensile and compressive loading was used as the cellular structure base material. The mechanical properties are listed in Table 4 and the constitutive model again accounted for strain rate sensitivity according to Eqn. (1).

Table 4. Mechanical properties of the polymer FullCure

	Young's modulus	Poisson's ratio	Yield stress	Cowper-Symonds' parameters	
	E	υ	Re	C	p
Tension	2,323 MPa	0.3	48.9 MPa	1,050 s^{-1}	3.5
Compression			91.0 MPa		

The cellular structure base material was discretised with 8-noded fully integrated quadratic solid elements. With additional parametric analyses the proper mesh density ($l \approx 0.1$ mm) and time step size ($\Delta t \approx 0.04$ μs) have been determined to assure precision of computational results. The cellular structure was loaded with displacement controlled compressive load at strain rate of 1,000 s^{-1}. Symmetry boundary conditions have been applied due to regular geometry of the cellular structure [34].

5.2 COMPUTATIONAL MODEL OF THE LIQUID FILLER

The viscous fluid filler was modelled with the Smoothed particle hydrodynamics method (SPH), where the analysed system state is represented by a set of particles (Figure 16). The particles possess individual material properties and move according to the governing conservation equations. The SPH method is a meshfree, Lagrangian, particle method [34, 40, 44, 45, 46].

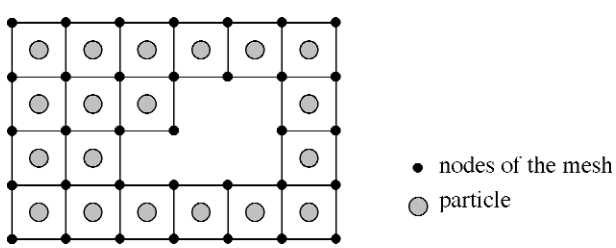

Figure 16 Domain discretisation with the finite element mesh and the mesh-free particles

The most significant is the adaptive nature of the SPH method, which is achieved by the field variable approximation (i.e. density, velocity, energy) that is performed at each time step based on the current local set of arbitrarily distributed particles. Because of the adaptive nature of the SPH approximation, the formulation of the SPH is not affected by the arbitrariness of the particle distribution. Therefore, it can handle problems with extremely large deformations without any difficulties. Another advantage of the SPH method is the combination of the Lagrangian formulation and particle approximation. Compared with Eulerian description, it is more effective, since only the material regions of interest need to be modelled, and not all the regions where material might exist. However, the SPH technology is relatively new compared to standard mesh-based Lagrangian and Eulerian descriptions, with remaining known problems in the areas of the stability, consistency and conservation [34, 45, 46].

Water (ρ = 1,000 kg/m^3 at 293 K) was used as the cellular structure filler in this study. The relationship between the change of volume and gas pressure has been represented with the Mie-Grüneisen equation of state [40, 44]. An optimal distance between the SPH particles ($l \approx 0.112$ mm) and mass of single particles ($m_i \approx 1.42$ µg) has been determined with separate parametric simulations.

The fully coupled interaction between the fluid filler and the cellular structure base material has been established using an automatic single surface contact algorithm [34, 40, 44].

The outflow of the liquid filler was validated and verified with the computational fluid dynamics code CFX [47]. It was confirmed that under compressive load approximately 96 % of the filler mass flow is in the horizontal direction of the open-cell cellular structure (Figure 17). Hence, only one layer of cellular structure was discretised and used in computational simulations, which essentially contributed to shorter and more reasonable computational times.

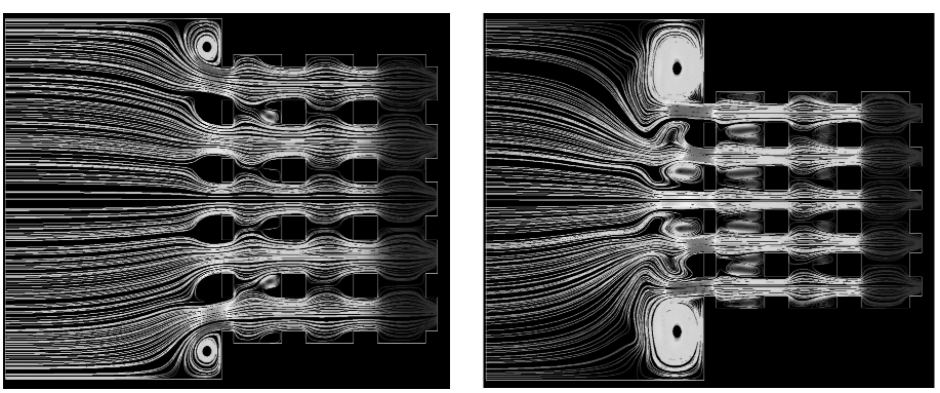

Figure 17 Streamlines of the filler during outflow

Figure 18 illustrates the comparison between the computational results obtained with the SPH model in the LS-DYNA code and the finite volume method using the ANSY CFX code.

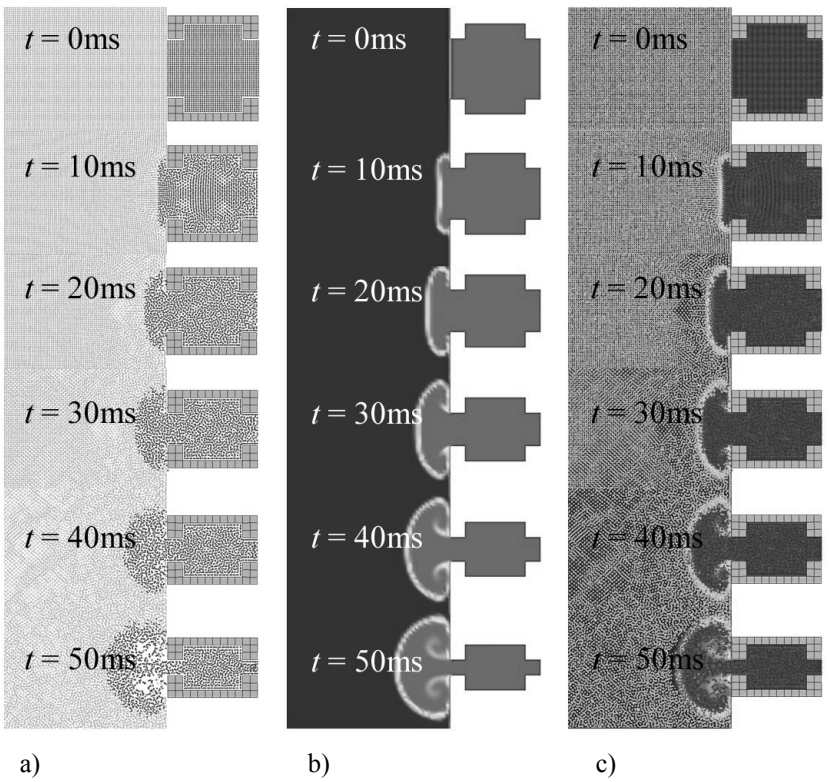

Figure 18 Filler outflow simulations: a) LS-DYNA (SPH model);
b) ANSYS CFX (finite volume method);
c) comparison between a) and b)

A very good agreement of results from both codes can be observed, which in turn validates suitability of the SPH model to accurately simulate the filler flow through the cellular material.

Described computational model has been used for parametric simulations to determine the influence of the fluid filler viscosity and its flow through the cellular structure, the size of cellular structure (number of cells) and the relative density. A single analysis run of the computational model with 16 cells lasted approximately 12 hours on a PC-cluster of 4 units with Intel Pentium IV 3200 MHz processors and 1 GB RAM each.

5.3 RESULTS

Figure 19 shows the deformation of the cellular structure with liquid filler under impact loading at different time sequences.

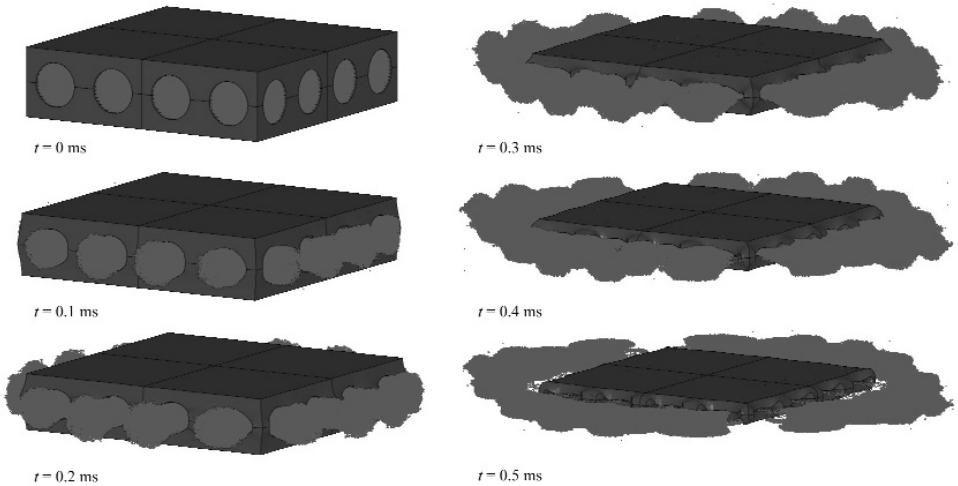

Figure 19 Deformation of the open cell-cellular structure accounting for fluid filler under impact loading

The computational simulations have confirmed that the size of the model and the number of the cells influence the macroscopic behaviour of cellular structure. Higher number of cells results in higher stiffness of the cellular structure and consequently in higher ability of energy absorption, since the filler is subjected to higher flow resistance and needs more time during its outflow, as shown in Figure 20.

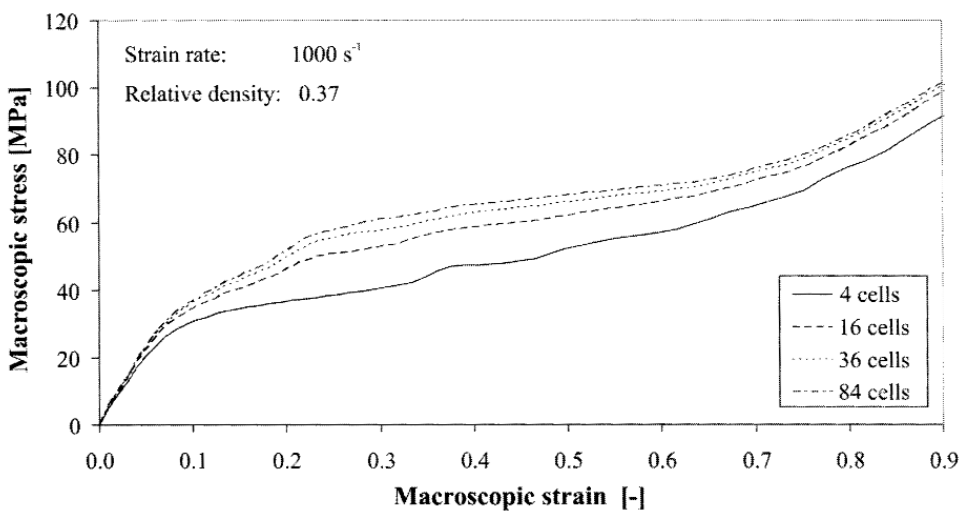

Figure 20 Influence of the cell number on cellular structure behaviour

Figure 21 illustrates the influence of the relative density and the filler. As already known, the stiffness increases with increasing the relative density. It can be also observed that the filler influences more the behaviour of cellular structure with higher relative density than the cellular structure with lower relative density. The reason for this effect can be derived from the fact that the filler is subjected to higher resistance during the outflow through the cellular structure with a high relative density, which consequently contributes to the increase of the macroscopic stiffness of the cellular structure.

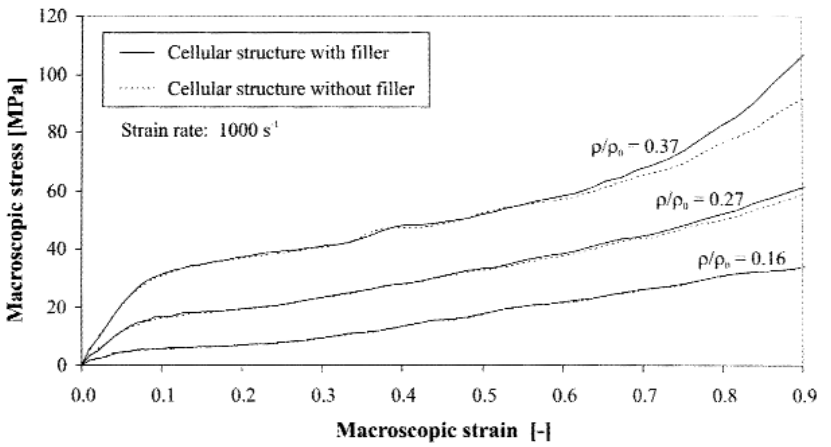

Figure 21 Influence of the viscous pore filler

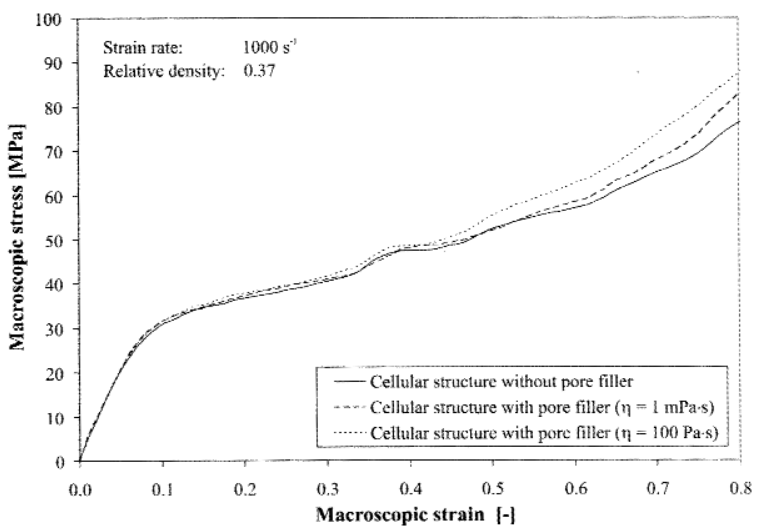

Figure 22. Influence of the pore filler viscosity

Figure 22 Influence of the pore filler viscosity

With further computational simulations it was also determined that the increase of the filler viscosity results in increase of macroscopic mechanical properties and consequently in higher stiffness of the cellular structure and higher capability of deformational energy absorption.

6 CONCLUSION

The paper discuses three very important fields of engineering computational simulations: (i) modelling of cellular structures, (ii) fluid-structure interaction and (iii) impact loading conditions.

To define the influence of several parameters on the behaviour of closed-cell cellular structure under impact conditions, computational model of the representative volume element has been developed. The influence of gas trapped in the pores has been studied in greater detail. The gas was described using an airbag model, accounting for the change of gas pressure, volume and temperature. Computational simulations have shown that the global stiffness of the cellular structure accounting for the gaseous fillers increases under compressive loading. However, the stiffness of such structures decreases under tensile loading. Consequently, the capability of crash energy absorption is higher under compressive loading. Higher internal pore gas pressure also results in densification at higher strains. It is determined that under higher internal pore gas pressure the cellular structure base material sustains higher plastic deformation. Computational results have also shown that the influence of the pore gas pressure increases with decrease of cellular structure relative density. The strain rate also affects the pore gas pressure. The influence of the internal pore gas pressure in considered cases is relatively small due to the high relative density that is determined with the cellular structure geometry ($\rho/\rho_0 > 0.48$). However, in commercial closed-cell cellular structures with much lower relative density ($\rho/\rho_0 < 0.1$), higher influence of the gaseous filler is expected. The influence of the gas type is negligible.

New models for fully coupled computational simulations of open-cell cellular structure with fluid fillers under impact conditions have been developed and evaluated. The fluid flow due to the cellular structure deformation is described with the smoothed particle hydrodynamics method. It was observed that the filler influences more the behaviour of cellular structure with higher relative density due to the cellular structure pore size effect. In cellular structure with high relative density the pore sizes are smaller than in cellular structure with lower relative density. Hence, the filler is subjected to higher resistance during the outflow in the first case, which consequently contributes to the increase of macroscopic stiffness of the cellular structure.

Future research work will be focused on experimental testing and also detailed study of cellular structure subjected to multi-axial impact loading conditions.

ACKNOWLEDGMENTS

Financial support of the Slovenian Research Agency (through contracts 3311-02-831229 and BI-PT-06-07-007) and the Slovenian Science Foundation is gratefully acknowledged.

REFERENCES

1. Cellular Metals and Polymers. Symposium, Fürth, 2004.
2. Austrian research centers – ARC. Ranshofen, 2005.
3. Jain V, Johnson I, Ganesh I, Saha BP, Mahajan YR. Effect of rubber encapsulation on the comparative mechanical behaviour of ceramic honeycomb and foam. Mater. Sci. Eng. A. 2003; 347; 109-122.
4. Körner C, Singer RF. Processing of metal foams – Challenges and Opportunities. Adv. Eng. Mater. 2000; 2(4): 159-165.
5. Banhart J. Manufacture, characterisation and application of cellular metals and metallic foams. Prog. Mater. Sci. 2001; 46(6): 559-632
6. Öchsner A, Tane M, Nakajima H. Prediction of the thermal properties of lotus-type and quasi-isotropic porous metals: Numerical and analytical methods. Mater. Lett. 2006; (60): 2690-2694.
7. Nakajima H, Hyun SK, Ohashi K, Ota K, Murakami K. Fabrication of porous copper by unidirectional solidaification under hydrogen and ist properties. Colloid. Surface. 2001; 197: 209-214.
8. Tane M, Ichitsubo T, Nakajima H, Hyun SK, Hirao M. Elastic properties of lotus-type porous iron: acoustic measurements and extended effective-mean-field theory. Acta Mater. 2004; 52: 5195-5201.
9. Andersen O, Waag U, Schneider L, Stephani G, Kieback B. Novel Metallic Hollow Sphere Structures. Adv. Eng. Mater. 2000; 2(4): 192-195.
10. Antoniou A, Onck PR, Bastawros AF. Experimental analysis of compressive notch strengthening in closed-cell aluminium ally foam. Acta Mater. 2004; 52: 2377-2386.
11. Gibson LJ, Ashby MF. Cellular solids: Structure and properties. Cambridge: Cambridge University Press; 1997.
12. Yu JL, Li JR, Hu SS. Strain-rate effect and micro-structural optimization of cellular metals. Mech. Mater. 2006; 38: 160-170.
13. Deshpande VS, Fleck NA. High strain rate compressive behaviour of aluminium alloy foams. Int. J. Impact Eng. 2000; 24(3): 277-298.
14. Sieradzki K, Green DJ, Gibson LJ (editors). Mechanical properties of porous and cellular materials. MRS proceedings. 1990.
15. Papadopoulos DP, Konstantindis IC, Papanastasiou N, Skolianos S, Lefakis H, Tsipas DN. Mechanical properties of Al metal foams. Mater. Lett. 2004; 58(21): 2574-2578.
16. Klein B. Innovativ Konstruieren mit neuen Werkstoffen und Leichtbau. Kassel: Universität Gesamthochschule Kassel; 2002.
17. Seitzberger M, Rammerstorfer FG, Gradinger R, Degischer HP, Blaimschein M, Walch. Experimental studies on the quasi-static axial crushing of steel columns filled with aluminium foam. Int. J. Solids Str. 2000; 37(30): 4125-4147.
18. Fusheng H, Jianning, Hefa C, Junchang G. Effects of process parameters and alloy compositions on the pore structure of foamed aluminium. J. of Mater. Process. Tech 2004; 138(1-3): 505-507.
19. Shapovalov VI. Porous metals. Mater. Research Soc. 1994; 19(4): 24-28.
20. NPL Workshop on Metallic Foams. The Sci. Museum National Physical Lab., 2000.
21. Ashby MF, Evans AG, Fleck NA, Gibson LS, Hutchinson JW, Wadley HNG. Metal foams: a design rule. Boston: Butterworth-Heinemann; 2000.
22. Metal foam info. Available online http://metalfoam.net [17.11.2004].
23. Gibson LJ. Biomechanics of cellular solids. J. Biomech. 2005; 38: 377-399.
24. Elzey DM, Wadley HNG. The limits of solid state foaming. Acta mater. 2001; 49: 849-859.
25. Öchsner A, Mishuris G, Gracio J, Modelling of the multiaxial elasto-plastic behaviour of porous metals with internal gas pressure, Elsevier Science Ltd, 2004.
26. Ohrndorf A, Schmidt P, Krupp U, Christ HJ. Mechanische Untersuchung eines geschlossenporigen Aluminiumschaums. Bad Nauheim: Deutscher Verband für Materialforschung und –prüfung, 2000.

27. Lankford J, Dannemann KA, Strain Rate Effects in Porous Materials, Mat. Res. Soc. Symp. Proc. Vol. 521, 1998.

28. Shkolnikov MB. Honeycomb modelling for side impact moving deformable barrier. 7th international LS-DYNA users conference, Dearborn, 2002.

29. Kitazono K, Sato E, Kuribayashi K. Application of mean field approximation to elastic-plastic behaviour for closed-cell foams. Acta mater. 2003; 51: 4823-4836.

30. Shim VPW, Yap KY, Stronge WJ. Effects of nonhomogeneity, cell damage and strain rate on impact crushing of a strain-softening cellular chain. Int. J. Impact Eng. 1992; 12: 585-602.

31. Shim VPW, Yap KY. Modelling impact deformation of foam-plate sandwich systems. Int. J. Impact. Eng. 1997; 19 (7): 615-636.

32. Picu CR, Vincze G, Öztürk F, Grácio J, Barlat F, Maniatty A. Strain rate sensitivity of the commercial aluminium alloy AA5182-O. Mat. Sci. Eng. A 2005; 390 (1): 334-343.

33. Vesenjak M, _uni_ Z, Öchsner A, Hriber_ek M, Ren Z. Heat conduction in closed-cell cellular metals. Mater. Sci. Eng. Tech. 2005; 36, (10): 608-612.

34. Vesenjak M. Computational modelling of cellular structures under impact conditions. Doctoral Thesis. Maribor: Faculty of Mechanical Engineering, 2006.

35. Altstädt V. Polymer Foams: Perspectives and Trends. 7th International workshop on advances in experimental mechanics, Portoro_, 2002.

36. Hanssen AG, Hopperstad OS, Langseth M, Ilstad H. Validation of constitutive models applicable to aluminium foams. Int. Journal Mech. Sci. 2002; 44 (2): 359-406.

37. Kouznetsova VG, Geers MGD, Brekelmans M. Multi-scale second-order computational homogenization of multi-phase materials: a nested finite element solution strategy. Comp. Method. Appl M. 2004; 193 (48-51): 5525-5550.

38. Reyes A, Hopperstad OS, Berstad T, Langseth M. Implementation of constitutive model for aluminium foam including fracture and statistical variation of Density. 8th international LS-DYNA users conference, Dearborn, 2004.

39. Öchsner A, Experimentelle und numerische Untersuchung des elasto-plastischen Verhaltens zellularer Modellwerkstoffe. Düsseldorf: VDI Verlag GmbH, 2003.

40. Hallquist J. Keyword manual. Livermore: Livermore Software Technology Corporation, 2003.

41. Altenhof A, Ames W. Strain rate effects for aluminum and magnesium alloys in finite element simulations of steering wheel impact test. Fatigue Fract. Engng. Mater. Struct. 2002; 25.

42. Bodner SR, Symonds PS, Experimental and theoretical investigation of the plastic deformation of cantilever beam subjected to impulse loading. J. Appl. Mech. 1962; 29.

43. Vesenjak M, Öchsner A, Ren Z. Behaviour of closed-cell foams under impact. Workshop on Computational Engineering Mechanics, Erlangen, 2005.

44. Hallquist J, Theoretical manual. Livermore: Livermore Software Technology Corporation, 1998.

45. Liu GR, Liu MB. Smoothed Particle Hydrodynamics – a meshfree particle method. Singapore: World Scientific, 2003.

46. Schwer LE. Preliminary Assessment of Non-Lagrangian Methods for Penetration Simulation, 8th International LS-DYNA User Conference, 2004.

47. CFX 5.6 user's manual. AEA Technology, 2003.